

THERMAL-MECHANICAL LIFE PREDICTION IN AFTER SHELL SECTION OF GAS TURBINE COMBUSTION LINER

Kyung Min Kim¹, Yun Heung Jeon¹, Namgeon Yun¹, Dong Hyun Lee¹, and Hyung Hee Cho^{1,*}

¹ Department of Mechanical Engineering

Yonsei University, Seoul, 120-749, Korea

(* Corresponding author: hhcho@yonsei.ac.kr)

High thermal efficiency of gas turbine systems is strongly related to the increase in the turbine inlet temperature, which is accompanied by the excess thermal load in the hot components of gas turbine. [Goldstein, 1971] Thus, various cooling techniques [Han et al., 2000] have been used to protect the main hot parts of the gas turbines. If an unsuitable cooling method is used, the local thermal crack and structural failure are yielded due to the thermal stress and the reduction of the material strength in high temperature. Therefore, the failure analyses as well as the thermal analyses for temperature, thermal stress, and life prediction are required for the effective thermal design of hot components. [Tinga et al., 2007; Kim et al., 2009]

In this paper, we can find the locations of high stresses under the base load operation using the thermal analysis of the after section of combustor liners. Moreover, we can predict the lifetime from thermal-mechanical stresses during the transient operations such as unit start-up and shut-down. Therefore, the objective of the present research is to find major causes of thermal damages affecting the lifetime induced by the temperature and thermal stress distributions.

The combustion liner in the present study is divided into three parts such as forward shell section, center shell section, and after shell section as shown in Fig. 1(a). Each section has different cooling methods. In other words, the forward shell, the center shell, and the after shell sections are cooled by rib-roughened passage, impingement jet, and C-channel, respectively. Among these sections, the after shell section is cooled using an internal passage cooling method because this section is inserted into transition piece. It is called C-channel and is invented by Intile et al. [2007]. The C-channel consists of cooling holes, divider walls, hot side wall, coolant side wall, and spring seals as described in Fig. 1(b). The simulated section is one hole segment of the 88 cooling holes because the shape has a symmetric behavior. The calculations of fluid flow and heat transfer are conducted using a computational fluid

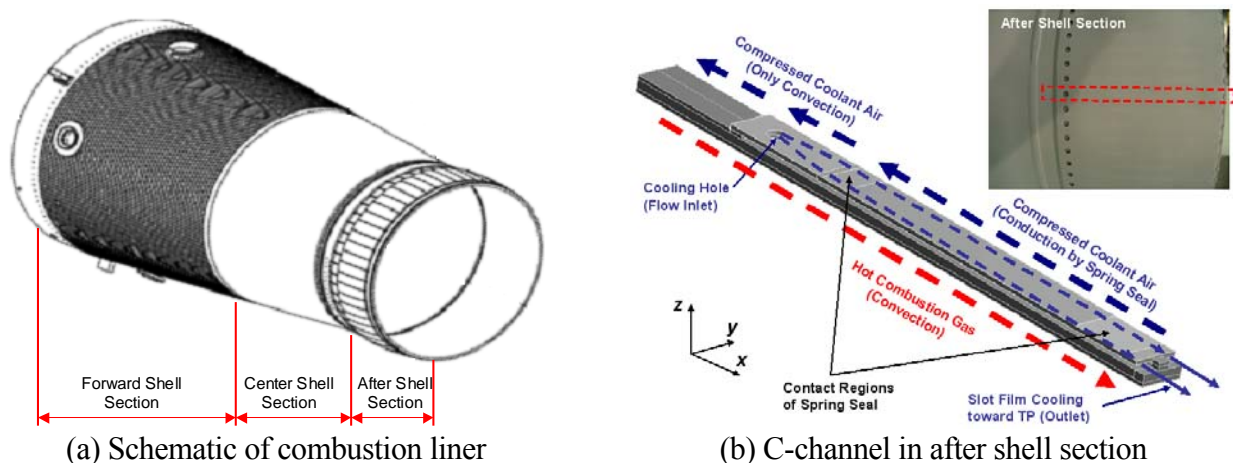


Figure 1. Geometries of the combustion liner

dynamics (CFD) code, CFX v11. The turbulence model is the SST $k-\omega$ model. The grid consists of approximately 1.5 million cells including flow and solid domains with TBC, of which thickness is 1.0 mm. A stress analysis was conducted using the calculated temperature data to find the causes of the thermal damage in the aforementioned geometries. The numerical stress analysis was performed using a finite element analysis (FEA) code, ANSYS v11. In the numerical calculations, the boundary conditions used the temperature and the heat transfer data calculated from the CFD analysis.

Figure 2 presents distributions of heat transfer coefficient and wall adjacent temperature under base-load operation in the internal passage called C-channel. The wall adjacent temperature (Fig. 2(a)) under the impinging hole is risen by 30°C more than the flow inlet temperature of 400°C due to the crossflow by the side wall nearby the welding region. The lowest wall adjacent temperature appears in the region between impingement jet hole and divider wall tip because the jet flow is deflected by the crossflow. The flow temperature increases as moving downstream from the hole and then it reaches up to 640°C on the hot side wall of the flow outlet. The temperature on the hot side wall is approximately 30°C higher than that on the coolant side wall. As shown in Fig. 2(b), the heat transfer coefficients are changed largely in the whole domain. In this whole domain, the distributions of heat transfer coefficients are divided into four different regions: (1) in the region of impingement jet and nearby side welding wall, the lowest heat transfer is obtained because of the interaction of the crossflow and the impinging jet; (2) in the region downstream of the impinging jet hole, heat transfer is enhanced significantly by the impingement of deflected jet flow. This flow yields the highest heat transfer coefficients in this region of the coolant side wall. Also, the heat transfer increases on the coolant side wall; (3) in the region after the tip of the divider wall, the impinged cooling flow is divided into two channels, and then the heat transfer coefficients are enhanced; (4) in the region downstream of the divider wall tip, the heat transfer rate is decreased slightly by the development of flow and thermal boundary layers.

Figure 3(a) shows the temperature distributions under base-load operation in the after section of the combustion liner. The characteristics of the temperature distributions are divided into four parts in the whole region. In Region 1, the temperature gradient is generated by only conduction between hot and cold regions. The maximum temperature appears at the end of the segment on TBC bottom and its magnitude is 915.85°C . In Region 2 (welding region), the temperature is ranged from 410°C to 520°C because the heat transfer is greatly affected by convection from region as well as conduction from Region 1. The temperature in Region 3 is decreased significantly up to 407.15°C in the x-axial direction because this coolant side wall is separated from hot side wall by the internal cooling channel. However, in Region 4, the contact between the two walls is made by the divider wall. Thus, the temperature reaches up to 630°C .

Figure 3(b) presents the thermal stresses resulting from the temperature distributions in Fig. 3(a). High thermal stresses on the coolant side wall appear in three local regions which are on the welding part of Region 2, nearby the hole in Region 3, and above the divider wall of Region 4. The high thermal stresses are caused by following reasons: (1) in the welding part of Region 2, the temperature gradient in the x-axial direction is decreased steeply by the cooling flow in the C-channel; (2) around the hole in Region 3, the thermal expansion rate is the lowest. However, the deformation in these regions is enforced due to high thermal expansion rate around high temperature metals, Thus, the thermal stress around the hole becomes bigger; (3) above the divider wall of Region 4, the thermal expansion rate on the coolant side wall is lower than that on the hot side wall, and then the deformation of the coolant side wall region is also influenced by the divider wall. Therefore, the high thermal stress is generated above the divider wall.

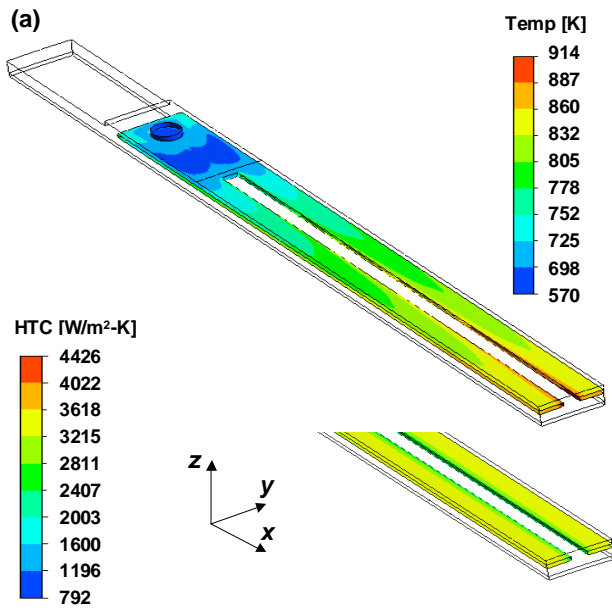


Figure 2. Flow and heat transfer analyses; (a) flow temperature, (b) heat transfer

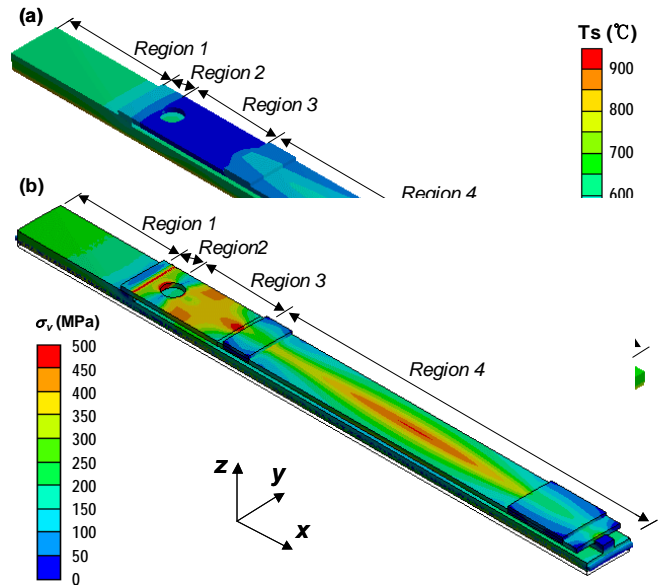
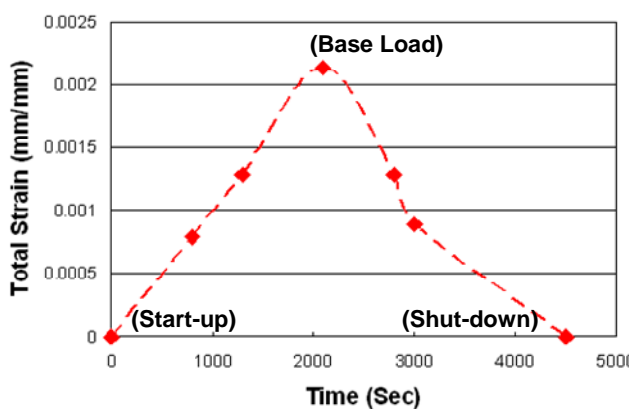


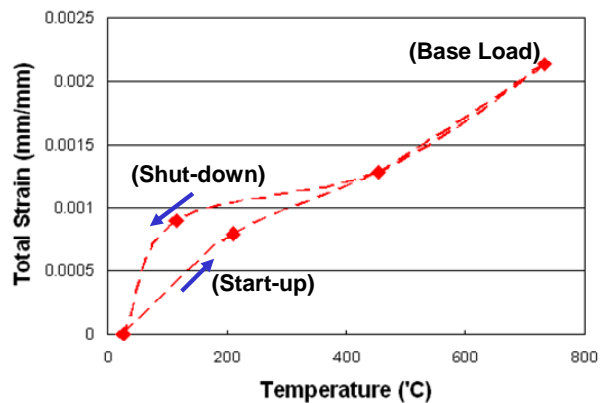
Figure 3. Thermal and mechanical analyses; (a) wall temperature, (b) thermal stress

Figure 4(a) shows strain variation under transient startup and shutdown operation. The strain distribution without TBC at the light-off step ranges from 9.5×10^{-6} to 1.4×10^{-3} . At the base load step, the strain distribution ranges from 1.4×10^{-5} to 4.6×10^{-3} . Strain range at each element during the transient operation has the maximum value at the base load operation and high thermal strains appear nearby the cooling hole and above the divider wall of the coolant side wall.

Figure 4(b) shows the strain-temperature variation of the element on the hot gas side. The minimum temperature distribution without TBC ranges from 31.1°C to 32.6°C at the light-off step and the maximum temperature distribution ranges from 405°C to 734°C at the base load step. The maximum temperature and strain imposed on the region are 733°C and 0.21% , respectively. The region is predicted to be the most vulnerable to TMF damage due to the maximum temperature in the after shell section in spite of low strain. This strain-temperature history at each element presents the information on TMF behavior suffered during the transient operation.



(a) Strain-time variation



(b) Strain-temperature variation

Figure 4. Strain-temperature variation on the hot gas side

CONCLUSION

In the present study, the failure analysis and the lifetime prediction were investigated from distributions of temperature and thermal stress in after shell section of gas turbine combustion liner. 3D-numerical simulations using the FEM and FVM commercial codes, ANSYS and CFX, were conducted to calculate distributions of temperature and thermal stresses in the C-channel, which protected this section connecting to a gas turbine transition piece.

The calculated temperature on the coolant side wall was lower than that on the hot side wall. The thermal deformation of the hot side wall is larger than that of the coolant side wall by the thermal expansion difference. The high thermal stresses resulting from the difference in thermal expansion were presented at three regions such as the welding region, around the hole, and the divider wall of C-channel. The calculated locations were similar to those of actual thermal cracks in combustion liner after section of gas turbine. In addition, the element on the divider wall with the highest stress is greatly affected by the thermal and mechanical stress under the start-up and shut-down operation.

REFERENCES

- Goldstein, R. J. [1971], Film Cooling, *Advances in Heat Transfer*, Vol. 7, pp. 321-379.
- Han, J. C., Dutta, S., Ekkad, S. V. [2000], *Gas Turbine Heat Transfer and Cooling Technology*, Taylor and Francis, New York.
- Intile, J. C., West, J. A., and Byrne W. [2007], Method and Apparatus for Cooling Combustion Liner and Transition Piece of a Gas Turbine, *United States Patent 2007*, No. US7010921 B2.
- Kim, K. M., Lee, D. H., and Cho, H. H. [2009] Thermal Analysis of a Film Cooling System with Normal Injection Holes Using Experimental Data, *International Journal of Fluid Machinery and Systems*, Vol. 2, pp. 55-60.
- Tinga, T., Kampen, J. F., Jager, B., and Kok, J. B. W. [2007] Gas Turbine Combustor Liner Life Assessment Using a Combined Fluid/Structural Approach, *ASME Journal of Engineering for Gas Turbines and Power*, Vol. 129, pp. 69-79.